IOPscience iopscience.iop.org

Home Search Collections Journals About Contact us My IOPscience

Hole magnetic polarons in zinc-blende semimagnetic semiconductors

This article has been downloaded from IOPscience. Please scroll down to see the full text article.

1997 J. Phys.: Condens. Matter 9 4289

(http://iopscience.iop.org/0953-8984/9/20/024)

View the table of contents for this issue, or go to the journal homepage for more

Download details:
IP Address: 171.66.16.207
The article was downloaded on 14/05/2010 at 08:44

Please note that terms and conditions apply.

J. Phys.: Condens. Matter **9** (1997) 4289–4302. Printed in the UK PII: S0953-8984(97)80217-2

Hole magnetic polarons in zinc-blende semimagnetic semiconductors

C Benoit à la Guillaume† and A K Bhattacharjee‡

† Groupe de Physique des Solides, URA au CNRS, Université Denis Diderot et Université Pierre et Marie Curie, 2 place Jussieu, 75251 Paris Cédex 05, France

‡ Laboratoire de Physique des Solides, URA au CNRS, Université Paris-Sud, Batiment 510, 91405 Orsay, France

Received 10 December 1996, in final form 5 March 1997

Abstract. A theory of hole magnetic polarons in diluted magnetic semiconductors of zinc-blende structure is presented, following the method introduced by Baldereschi and Lipari to solve the neutral acceptor problem. An expression for the nonlinear magnetic potential is determined in the mean-field approximation. An efficient numerical method is used to solve the system of two coupled differential equations. Results are presented for quantum dots, neutral acceptors and free magnetic polarons. The present theory predicts a substantial increase of the magnetic polaron energy in all cases. An excellent parameter-free fit of acceptor magnetic polaron energy versus temperature is obtained for diluted systems. Simplified models based on a single parabolic band with two adjustable parameters, the hole mass and the exchange integral, are shown to be inadequate, in particular in the case of quantum dots.

1. Introduction

In semimagnetic or diluted magnetic semiconductors (DMSs), one topic which has been well studied, both experimentally and theoretically, is the magnetic polaron (MP) [1], which arises from strong sp–d exchange interaction between a band carrier and the magnetic ions. Strong MPs are related mainly to holes (neutral acceptors or localized excitons), since p–d exchange is usually about four times stronger than s–d exchange, at least in II–VI compounds. In zinc-blende material, the degeneracy at the top of the valence band of Γ_8 symmetry makes the theory more complicated. This is why, in MP models, holes are usually treated as simple parabolic-band particles with $\frac{3}{2}$ effective spin, characterized by two parameters, m_h the effective mass and $\beta' = \rho\beta$, the exchange parameter [2], where β is the exchange constant for a free hole. The factor ρ, smaller than unity, arising from hole localization, was first calculated for a uniform exchange field in an acceptor [3] and in a quantum dot (QD) [4].

In this paper, we present a more precise treatment for zinc-blende semiconductors, based on the spherical model introduced by Baldereschi and Lipari (BL) [5] to solve the shallow-acceptor problem. In section 2, we derive an expression for the magnetic potential in the mean-field approximation. The procedure of numerical solution for the two BL coupled differential equations is described in appendix A. Results for a hole MP in a QD are presented in section 3. We show that standard calculations give the same result only at saturation. Away from saturation, the present theory gives a sizeable increase in MP energy, by a factor that can be of the order of two. We show in appendix B how a new

0953-8984/97/204289+14$19.50 © 1997 IOP Publishing Ltd

factor $\eta > 1$ has to be substituted for ρ in the high-temperature linear regime. In section 4, results for a neutral acceptor MP are given. Extension to a free MP is also outlined.

2. Theory

In the spherical approximation for the Luttinger Hamiltonian, the hole wavefunctions are

$$\Psi_\kappa(\boldsymbol{r}) = \sum_\nu F_{\nu\kappa}(\boldsymbol{r}) u_\nu(\boldsymbol{r}) \tag{1}$$

where κ and ν run through $\frac{3}{2}$, $\frac{1}{2}$, $-\frac{1}{2}$ and $-\frac{3}{2}$. $u_\nu(\boldsymbol{r})$ are the time reversed valence band Bloch functions at Γ. Note that, following BL and Efros [6], we have included the fourfold Γ_8 valence band only in (1). Recently, Richard *et al* [7] have reported that the contribution from the spin–orbit split-off band Γ_7 might be of crucial importance for the QD hole level ordering. Here, we consider the fourfold ground state $1S_{3/2}$ that corresponds to

$$F_{\nu\kappa}(\boldsymbol{r}) = \delta_{\nu\kappa} R_0(r) Y_{00} + \langle \tfrac{3}{2}, \nu; 2, (\kappa - \nu) | \tfrac{3}{2}, \kappa \rangle R_2(r) Y_{2,\kappa-\nu}(\theta, \varphi) \tag{2}$$

where Clebsch–Gordan coefficients have been used. Let us rewrite the radial functions $R_0(r)$ and $R_2(r)$ as

$$f(r) = (4\pi)^{-1/2} R_0(r) \qquad g(r) = (4\pi)^{-1/2} R_2(r) \tag{3}$$

which satisfy the normalization condition

$$\int_0^\infty 4\pi r^2 [|f(r)|^2 + |g(r)|^2] \, \mathrm{d}r = 1. \tag{4}$$

As pointed out by BL, the above functional form (2) remains valid in any potential of spherical symmetry. Unperturbed QD functions $f(r)$ and $g(r)$ can be written in terms of spherical Bessel functions [6].

Now, the expectation value of the exchange interaction between the hole and the Mn d electrons (total ionic spin $S = \frac{5}{2}$) is given by [4]

$$\langle H_{exc} \rangle_\kappa = -\frac{\beta}{3} \sum_{i,\lambda,\xi} F^*_{\lambda\kappa}(\boldsymbol{R}_i) \langle \lambda | \boldsymbol{j} \cdot \boldsymbol{S}_i | \xi \rangle F_{\xi\kappa}(\boldsymbol{R}_i) \tag{5}$$

where i labels the Mn ion sites and β is the p–d exchange constant. The effective exchange field acting on an Mn spin at $\boldsymbol{r}$ is thus

$$\boldsymbol{B}_{eff}(\boldsymbol{r}) = \frac{\beta}{3 g \mu_B} \sum_{\lambda,\xi} F^*_{\lambda\kappa}(\boldsymbol{r}) \langle \lambda | \boldsymbol{j} | \xi \rangle F_{\xi\kappa}(\boldsymbol{r}). \tag{6}$$

Note that this exchange field contains an angular dependence even if we neglect its transverse components. In order to restitute the spherical symmetry of our problem, we average over the orientation $\boldsymbol{r}$ in (6), so that the effective field along the mean-field axis $\boldsymbol{z}$ reads

$$B_{eff}(r) = \frac{\beta}{g \mu_B} \kappa (|f(r)|^2 + \tfrac{1}{5}|g(r)|^2). \tag{7}$$

The magnetic free energy can be written as

$$G_{mag} = -\int \mathrm{d}\boldsymbol{r} \int_0^{B_{eff}(\boldsymbol{r})} M(B) \, \mathrm{d}B \tag{8}$$

where $M(B)$ is the magnetization of the Mn spin system (assumed to be continuous). The total free energy of the hole and the magnetization cloud is

$$G = G_{mag} + T_h + V_{ext}. \tag{9}$$

T_h and V_{ext} are respectively the expectation values of the hole kinetic energy and of the non-magnetic potential energy $V(r)$ (like the Coulomb potential in the acceptor case).

According to BL for a $1S_{3/2}$ state

$$T_h = -\frac{\hbar^2}{2m_0}\gamma_1\left[\int \mathrm{d}\boldsymbol{r}\, f^*(r)\left\{\left[\frac{\mathrm{d}^2}{\mathrm{d}r^2}+\frac{2}{r}\frac{\mathrm{d}}{\mathrm{d}r}\right]f(r)-\mu\left[\frac{\mathrm{d}^2}{\mathrm{d}r^2}+\frac{5}{r}\frac{\mathrm{d}}{\mathrm{d}r}+\frac{3}{r^2}\right]g(r)\right\}\right.$$
$$\left.+\int \mathrm{d}\boldsymbol{r}\, g^*(r)\left\{-\mu\left[\frac{\mathrm{d}^2}{\mathrm{d}r^2}-\frac{1}{r}\frac{\mathrm{d}}{\mathrm{d}r}\right]f(r)+\left[\frac{\mathrm{d}^2}{\mathrm{d}r^2}+\frac{2}{r}\frac{\mathrm{d}}{\mathrm{d}r}-\frac{6}{r^2}\right]g(r)\right\}\right]. \quad (10)$$

Here, m_0 is the free electron mass and μ the BL parameter defined as

$$\mu = (4\gamma_2 + 6\gamma_3)/(5\gamma_1)$$

in terms of the Luttinger parameters γ_i. V_{ext} is simply $\langle f(r)|V(r)|f(r)\rangle + \langle g(r)|V(r)|g(r)\rangle$.

The usual variational recipe for minimization reads

$$(\partial/\partial f^*)(G - EN) = 0 \qquad (\partial/\partial g^*)(G - EN) = 0 \quad (11)$$

where N and E represent the norm and the Lagrange multiplier respectively. We thus arrive at a system of two coupled Schrödinger equations:

$$-\frac{\hbar^2\gamma_1}{2m_0}\left[\left\{\frac{\mathrm{d}^2}{\mathrm{d}r^2}+\frac{2}{r}\frac{\mathrm{d}}{\mathrm{d}r}\right\}f(r)-\mu\left\{\frac{\mathrm{d}^2}{\mathrm{d}r^2}+\frac{5}{r}\frac{\mathrm{d}}{\mathrm{d}r}+\frac{3}{r^2}\right\}g(r)\right]$$
$$+\{V_{mag}+V(r)-E\}f(r)=0 \quad (12a)$$
$$-\frac{\hbar^2\gamma_1}{2m_0}\left[\left\{\frac{\mathrm{d}^2}{\mathrm{d}r^2}+\frac{2}{r}\frac{\mathrm{d}}{\mathrm{d}r}-\frac{6}{r^2}\right\}g(r)-\mu\left\{\frac{\mathrm{d}^2}{\mathrm{d}r^2}-\frac{1}{r}\frac{\mathrm{d}}{\mathrm{d}r}\right\}f(r)\right]$$
$$+\{\tfrac{1}{5}V_{mag}+V(r)-E\}g(r)=0 \quad (12b)$$

where

$$V_{mag}(r) = -(\beta\kappa/3g\mu_B)M(B_{eff}(r)) \quad (13)$$

with B_{eff} from (7). For the local magnetization functional, we can use, following [8], the experimental high-field magnetization curve [9]:

$$M(H) = g\mu_B N_0 x_{eff}(\tfrac{5}{2})B_{5/2}(5g\mu_B H/2k(T+T_0)) + \alpha_l H. \quad (14)$$

N_0 is the density of cation sites, x_{eff} the concentration of 'free' magnetic ions, T_0 a parameter taking into account the mean long-range antiferromagnetic interaction between ions and $B_{5/2}$ the Brillouin function for spin $\frac{5}{2}$. The linear term $\alpha_l H$, where α_l is an empirical parameter, partly represents cluster contributions that cannot be described by the modified Brillouin function. This term is important for small QD where the effective field B_{eff} in (7) may reach several tens of tesla.

Let us note that (12*a*) and (12*b*) are just the generalization for the MP case of (27*a*) of BL. In [5], the system of differential equations (12*a*, *b*) was solved variationally, $f(r)$ and $g(r)$ being developed as a sum of Gaussian functions. Here, we introduce a new method of numerical solution of the system (12*a*, *b*), which is explained in appendix A. We have checked the accuracy of this method in two ways: (i) we obtained for the acceptor case results in very good agreement with those of BL; (ii) in the case of the localization energy of a hole in a spherical QD with infinite barrier, an analytical solution exists [6], $f(r)$ and $g(r)$ being combinations of spherical Bessel functions; here again, our numerical solution is excellent.

3. A hole MP in a QD

Calculations are performed for a semimagnetic $Cd_{1-x}Mn_xTe$ QD of radius R. We consider a hole MP in order to exhibit more clearly the difference with the simplified model assuming a simple parabolic hole band. The CdTe material parameters used are listed in table 1 and the magnetic parameters [9] for CdMnTe in table 2. We have used the set of γ_i from [11], deduced from cyclotron resonance for different crystallographic orientations and from the exciton centre of mass quantization in wide quantum wells; it provides also a reasonable value of acceptor binding energy, 58 meV, close to experimental data, while the Lawaetz parameters [10] give 87 meV. For the MP ground state, we have to choose $|\kappa| = \frac{3}{2}$ in (13) for $V_{mag}(r)$. Figure 1 shows the temperature dependence of the polaron energy for QDs of radius 2 nm, with $x = 5$ and 10% and a magnetization described by (14); for $x = 5\%$, the linear term in (14) is negligible.

Table 1. Material parameters of CdTe. N_0 is the density of cation sites, ε the static dielectric constant, γ_i the Luttinger parameters of the valence band according two different authors and μ the corresponding BL parameter.

$N_0 = 1.47 \times 10^{-22}$ cm^{-3}			$\varepsilon = 10$	
Ref.	γ_1	γ_2	γ_3	μ
[10]	5.29	1.89	2.46	0.844
[11]	4.7	1.45	1.9	0.732

Table 2. Magnetic parameters of $Cd_{1-x}Mn_xTe$ (α_l is in erg G^{-2} cm^{-3}).

$N_0\beta = -0.88$ eV			
x (%)	x_{eff} (%)	T_0 (K)	α_l
5	3.05	2.2	~ 0
10	3.8	2.5	0.22×10^{-4}
14	3.8	2.9	0.5×10^{-4}

We show also the results of the simplified model, i.e. the numerical solution of a single non-linear Schrödinger equation:

$$-(\hbar^2/2m_0m_h)(\mathrm{d}^2/\mathrm{d}r^2 + (2/r)\mathrm{d}/\mathrm{d}r)\Phi_h(r) + (V_{mh}(r) - E_h)\Phi_h(r) = 0 \quad (15)$$

where

$$V_{mh}(r) = -(\beta'/2g\mu_B)M((\beta'/2g\mu_B)|\phi_h(r)|^2) \qquad (\Phi_h(r) \text{ normalized}) \quad (16)$$

$m_h = E_{loc}(0)/\gamma_1 E_{loc}(\mu)$ is chosen in order to obtain the correct localization energy $E_{loc}(\mu)$ and the effective exchange parameter β' is taken as $\rho\beta$ where the *reduction* factor reads [4]

$$\rho = \int_0^R 4\pi r^2[|f(r)|^2 + \tfrac{1}{5}|g(r)|^2]\,\mathrm{d}r. \quad (17)$$

In figure 1, a good agreement between the two calculations is obtained only for $x = 5\%$ and T close to zero, i.e. when saturation is achieved over the whole QD. For $x = 10\%$, saturation is not achieved at $T = 0$ due to the linear term in (14). In the high-temperature region, considerable discrepancy is observed, the present calculation giving much higher

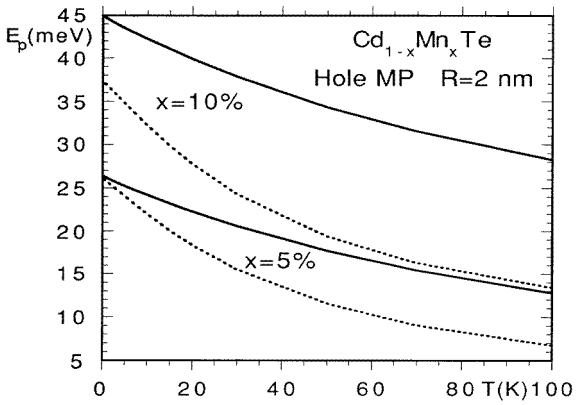

Figure 1. Hole MP energy versus temperature for a $Cd_{1-x}Mn_xTe$ QD of radius $R = 2$ nm for compositions $x = 5$ and 10%. The full curves give the results of the present model and the dotted lines the results from the simplified model (15).

values for the MP energy, by a factor of the order of two. We discuss below the physical origin of such a large discrepancy.

Let us recall that the value of ρ is obtained under the assumption of a uniform exchange field acting on the hole [3, 4], such a situation being approached in the MP case only at saturation. In the opposite limit, in the weak-coupling regime at high temperature, the exchange potential acting on the hole becomes proportional to $B_{eff}(r)$ (7) and, thus, varies rapidly with r. We find that the variation of the polaron energy in the linear regime is obtained by using $\beta' = \eta\beta$ where η is an *enhancement* factor. In the first order of perturbation (see appendix B), we obtain

$$\eta = \int_0^R 4\pi r^2[|f(r)|^2 + \tfrac{1}{5}|g(r)|^2]^2\,\mathrm{d}r \Big/ \int_0^R 4\pi r^2|f_0(r)|^4\,\mathrm{d}r \tag{18}$$

$f_0(r)$ being the wavefunction for $\mu = 0$. Indeed, η given by (18) is in good agreement with the full numerical calculation using a small magnetic potential (see figure 2), except for $\mu > 0.8$, the numerical result being 10% higher for $\mu = 0.95$. ρ and η are shown in figure 2 as functions of the BL parameter μ (see also table 3). When μ increases from zero to unity, ρ decreases from 1 to 0.6; ρ describes the variation with μ of the polaron energy at saturation. In contrast, η increases from 1 to a maximum of 1.52 for $\mu = 0.72$ and then deceases towards 1. η describes the variation with μ of the polaron energy in the linear regime. Thus, the strong enhancement of the MP energy in the present model is shown to arise from the spatial variation of the exchange field. This is the main new and unexpected result which explains the gross behaviour of MP energy away from saturation. η may be considered as a form factor. Let us point out that ρ and η were computed in (17) and (18) with the unperturbed $f(r)$ and $g(r)$ functions (i.e. in the absence of the MP effect). More subtle effects arise from the T dependent modification of $f(r)$ and $g(r)$ when the magnetic potential is included (see figure 3).

We can conclude that hole MP energy in a zinc-blende QD is underestimated in a significant way by the usual simplified theory. Experimental data on an MP in a QD are expected to be related to the exciton (even if such data in CdMnTe are not yet available). Since the contribution from the hole to the exciton MP energy is of the order of $\frac{2}{3}$, a

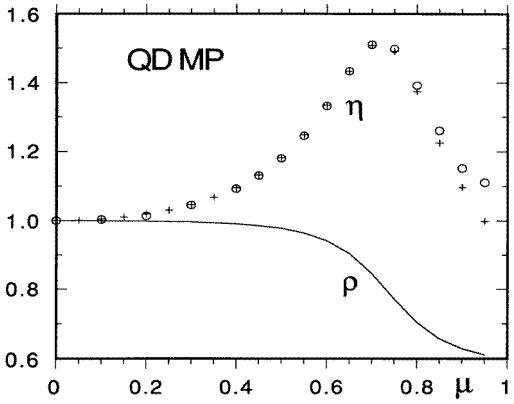

Figure 2. For a QD, μ dependence of the factors ρ (full line) corresponding to the saturation limit and η (+ from (18) and ○ from numerical calculation) representing the high-temperature linear regime.

Table 3. The parameters ρ, η and m_h corresponding to the γ_i set of [11] for a QD and A^0.

	ρ	η	m_h
QD	0.798	1.51	0.278
A^0	0.804	7.79	0.432

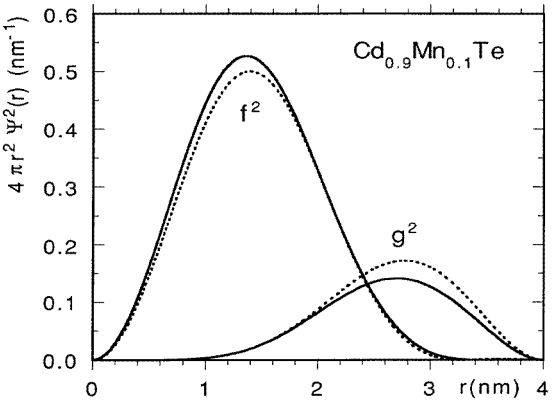

Figure 3. Radial probability density for f and g envelopes for $R = 4$ nm: dotted curves, the free hole $1S_{3/2}$ state; full curves, the MP case with $x = 10\%$ and $T = 2$ K.

significant increase in exciton MP energy is expected. The new treatment of the exciton MP in a QD will be published elsewhere [12].

We can already foresee corrections to the present results due to the fact that magnetic ions near the QD surface have fewer neighbours than those in the bulk. This could be taken into account by using a magnetization M function of H and r. However, from the shape of the hole wavefunction shown in figure 3, we can expect these corrections to be rather small, since, near the surface, the $g(r)$ envelope dominates, with a reduced magnetic coupling $V_{mag}/5$ in (12*b*).

4. Further applications

4.1. The A^0 MP

The neutral acceptor MP can be revisited with our new method. The effect on the linear regime described by the parameter η of (18) is even more drastic, as shown in figure 4. This is because, in this case, $f(r)$ remains close to an exponential function, with an effective Bohr radius shrinking to zero as μ approaches unity, approximately as $(1-\mu^2)$.

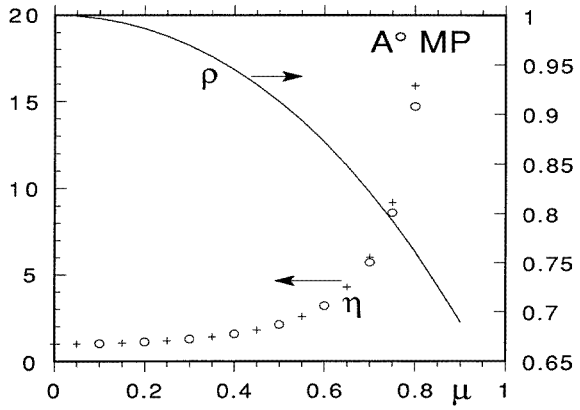

Figure 4. The μ dependence of the factors ρ (full line) and η (+ from (18) and ○ from numerical calculation) for a neutral acceptor.

The temperature dependence of the polaron energy in $Cd_{1-x}Mn_xTe$ for $x = 5\%$ is shown in figure 5. This result is first compared with experiments [13]. As can be seen in figure 5, the fit of the temperature dependence of the MP energy is nearly perfect. Let us stress that this is the first *parameter free* theory. For comparison, we show also the result of the simplified theory ((15) where the Coulomb attraction was added). We have used a reduced value of the exchange constant, $\beta' = \rho\beta$ with ρ given by (17) (see table 3). This simplified model is equivalent to the Ram-Mohan–Wolff model [8] (however, no reduction factor was considered in [8]). The fit of the simplified model is obviously poor, even at low T, and the discrepancy increases with increasing T. By comparison with the QD case ($x = 5\%$ and $R = 2$ nm) of figure 1, the saturation in the acceptor case is achieved only in a fraction of the wavefunction, near the centre. The rather different model which takes into account magnetic fluctuations as well as discrete space distribution of Mn ions, presented in [13], involves two fitting parameters, the value of ρ which fixes essentially the low-T value of the MP energy and a cut-off radius which fixes the high-T behaviour. The remaining incertitude in the present calculations based on the BL work stems from the lack of accuracy in the Luttinger parameters γ_i. In fact, we have checked that the relevant parameter which governs the high-T behaviour is μ (see in figure 5 the dashed curve, which corresponds to $\mu = 0.8$); this was also demonstrated by the μ dependence of η shown in figure 4.

The same treatment is presented for $x = 10\%$ and $x = 14\%$ in figure 6. Obviously, the fit of the MP energy is no longer good, the experimental points being about 15 meV higher than the theory. Let us recall that in [13] and [14] the MP energy was obtained neglecting any variation with x of the acceptor binding energy E_b, in the absence of MP effect. However, in this range of composition, the direct band gap of the material is larger by at least 10%, so a sizeable decrease of the dielectric constant and some increase of the hole effective mass

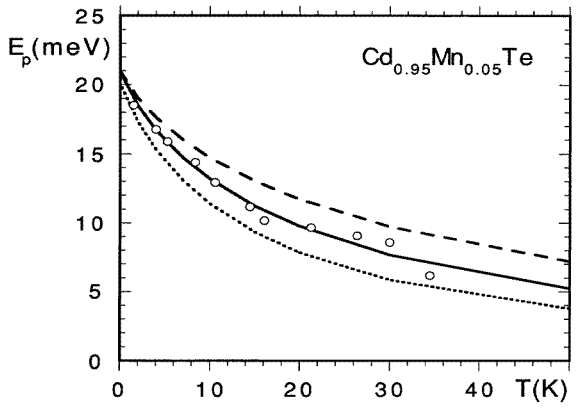

Figure 5. Temperature dependence of MP energy of the neutral acceptor in CdMnTe for $x = 5\%$. ○, experimental data from [14]. The present theory is given by the full curve for $\mu = 0.732$ and by the dashed curve for $\mu = 0.8$; the dotted curve is the result of the simplified model ($\rho = 0.804$ and $m_h = 0.432$).

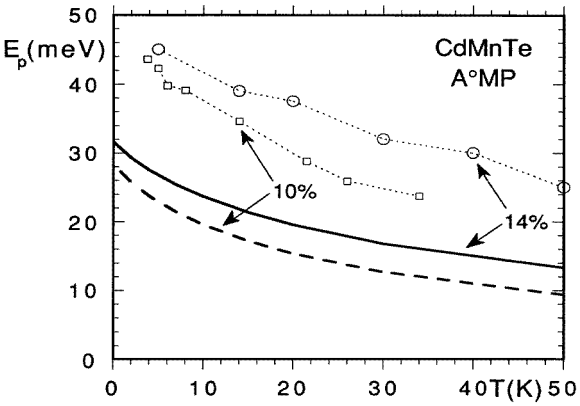

Figure 6. Temperature dependence of MP energy of the neutral acceptor for $x = 10\%$ (experimental data from [14] (□) and present theory (dashed line)) and for $x = 14\%$ (experimental data from [15] (○) and present theory (full line)).

are expected and, consequently, an increase of E_b that might explain part of the discrepancy. Let us remark also that the results of the simplified model (not shown in figure 6) are about 20% lower than the $T = 5$ K point computed in [8]. This is clearly because the N_0J ($N_0\beta'$ in this work) value used by the authors of [8] was 0.88 eV, the free hole value. Another contribution to the observed discrepancy might originate from the rather strong gradient of the exchange field $B_{eff}(\boldsymbol{r})$ acting on small ion clusters, as suggested in [15], where the degeneracy at the top of the valence band was taken into account. However, while the contribution of nearest-neighbour pairs is rather easily evaluated, calculation of these gradient terms for $x > 10\%$ seems very difficult.

Finally, let us discuss briefly the somewhat different behaviour of MPs in a QD and A^0 according to the present model. It can be traced back to the better uniformity of hole spatial distribution in a QD. For that reason, we can clearly approach in a small QD the two limiting cases: saturation, governed by the ρ factor, at low T, and the linear regime,

ruled by the η factor, at high T. In contrast, these two limits are never clearly obtained in neutral acceptors, due to the very non-uniform hole wavefunction.

4.2. The free hole magnetic polaron

We consider now the case of a free hole MP in zinc-blende semiconductors as an addition to the work of [16], where a simple parabolic band was assumed. As in [16], we use a dimensionless coupling parameter λ to express the strength of the exchange interaction between the hole and the magnetic ions [17]. In this case, the procedure described in appendix A is modified as follows: we fix the energy E and we have two unknowns, $\zeta = f(0)$ and $\alpha = g(\delta)/\zeta$. $B_{eff}(r)$ is computed according to (7), $f(r)$ and $g(r)$ being *not normalized*. So, the magnetic potential $V_{mag}(r)$ can be computed at each step. Once the conditions $F \to 0$ and $G \to 0$ are obtained [18], λ is determined from the normalization of $f(r)$ and $g(r)$. Then, the free energy F is computed by integration. Let us remark that the function $\lambda(E)$ is always single valued, but the function $E(\lambda)$ is not, in particular, when one unstable branch of solution exists. If we fix λ first, the unstable branch is not obtained. The energy E and free energy F (in reduced units) are displayed in figure 7 for $\mu = 0.6$ versus the coupling constant λ. The general aspect of these curves is not modified qualitatively with respect to figure 1(c) of [16], but the numerical values of λ, E and F at specific points depend on μ. Let us discuss more precisely the comparison between the present model and the simplified model; the results for the latter can be deduced from [16] by an appropriate scaling. In these caculations in terms of the coupling parameter λ, we have used an energy unit $U_s = (N_0\beta/2)\frac{5}{2}x_{eff}$, the polaron energy at saturation and a length unit d_s such that $U_s = \bar{h}^2/2m_0m_hd_s^2$. The expression giving the dimensionless λ parameter is [17] $\lambda = \frac{7}{12}\beta/k_B(T + T_0)d_s^3$. In the present calculation, we use β and $m_h = 1/\gamma_1$, but in the simple model, we use $\beta' = \rho\beta$ and a value of m_h we shall discuss later. So, we can deduce the result of the simple model (with the same reduced units as in the present model) from figure 1(c) of [16] by the following scaling: $E \to \rho E$ and $\lambda \to (\gamma_1 m_h)^{-3/2}\rho^{-5/2}\lambda$. This is shown in figure 8 for $\mu = 0.8$. The result of the simplified model (dotted curve) is deduced from the copy of figure 1(c) of [16] (dashed curve) through the scaling indicated by the arrow. The value $\rho = 0.77$ was deduced from $\langle f|f\rangle$ and $\langle g|g\rangle$ in the present calculation for λ in the $(\lambda^*, \lambda^{**})$ range. For m_h, we have taken arbitrarily the value for the A^0 case, i.e. $\gamma_1 m_h = E_b(0.8)/E_b(0) = 2.58$. A comparison between the full and dotted curves in figure 8 shows clearly that the present model predicts a larger polaron energy. Also the λ^* value which marks the limit between metastable and unstable free MP states is reduced by a factor of 1.5 (or the value $(T^* + T_0)$ corresponding to λ^* is increased by the same factor).

4.3. Comparison with related works

The authors of [19] considered free hole MP in the two limits $\mu = 0$ and $\mu = 1$. They performed the minimization of the free energy using a one-parameter trial wavefunction of Gaussian shape. Their results for $\mu = 0$ can be readily compared to the exact numerical calculations of [16], noting the relation between their B_1 parameter and the λ coupling parameter: $B_1^3\lambda^2 = 334.6$. Indeed, the behaviour of E and F near saturation is the same, but we can estimate the error due to the one-parameter minimization by comparing the results for the point where the MP loses its stability ($F = 0$): in figure 2 of [19] this happens for $B_1^{3/5} = 0.43$ (corresponding to $\lambda = 151$) for $E = 0.44$. The exact result is $\lambda = 124$ for $E = 0.2$.

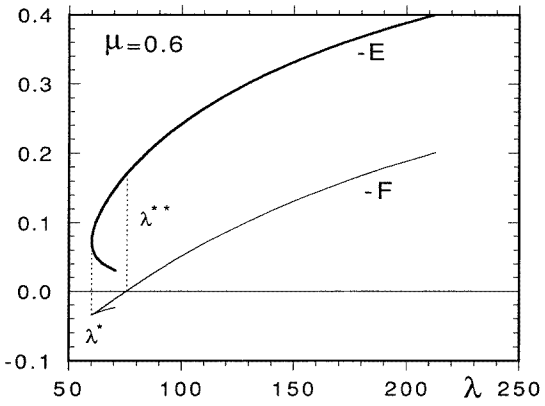

Figure 7. The energy E and free energy F, in reduced units, of a free hole MP versus λ for $\mu = 0.6$.

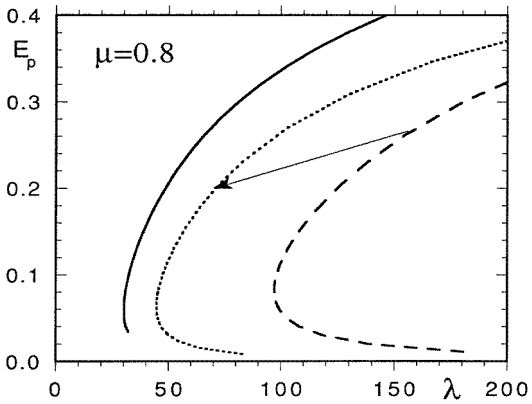

Figure 8. The polaron energy of a free hole MP for $\mu = 0.8$. The full curve is the present result. The dashed curve is figure 1(c) of [16]. The dotted curve, obtained from the latter by an appropriate scaling (see the text), is the result of the simplified model.

In [19] for the $\mu = 1$ limit, a finite heavy hole mass m_{hh} was assumed (so that $m_{lh} = 0$). In this limit, replacing m_0/γ_1 by $m_{hh}(1 - \mu)$, the system of equations (12a, b) becomes homogeneous because of the factor $(1 - \mu)$ mutiplying the E and V terms. By a linear combination of the two equations, $g(r)$ is related to $f(r)$ by the relation $(\mathrm{d}/\mathrm{d}r)f(r) = (\mathrm{d}/\mathrm{d}r + 3/r)g(r)$ which is the same as (14) of [19]. With $f(r)$ taken as a Gaussian, the results of the minimization look reasonable: in particular, the ratio of the MP energies at saturation $E_{sat}(\mu = 0)/E_{sat}(\mu = 1) = 0.56$ is close to our value of ρ for $\mu = 1$. However we may have some doubts about their validity, for the following reason: we can find a solution of the homogeneous system for a spherical QD of radius $R_0(f(u) = 1 - (8u - 5u^2)/3$, $g(u) = -2(u - u^2)/3$ with $u = r/R_0)$ but no solution going smoothly to zero at large r could be found in free space. This suggests that there is no well behaved $\mu = 1$ limit for bound states such as the neutral acceptor, A^0, MP or the free hole MP in free 3D space.

The authors of [20] claim that a hole MP in zinc-blende material is anisotropic, even when $\gamma_2 = \gamma_3$. It is not clear what they mean by anisotropy in this case. Apparently,

they mean to emphasize that the spatial distribution of the hole moment is of axial rather than spherical symmetry, as can be seen from our equation (6), but the MP axis in this case has no preferential direction with respect to the crystal axis. On the other hand, when $\gamma_2 \neq \gamma_3$, a true anisotropy is expected to arise from the term of cubic symmetry in the Luttinger Hamiltonian. Indeed, the authors of [20] conclude that, for $\gamma_3 > \gamma_2$, the optimal MP orientation is along the body diagonal. This anisotropy is not considered in our present treatment. The anisotropy is, however, most important in wurtzite-structure materials [21].

5. Conclusion

We have adapted for the MP problem the BL method [5] to treat bound hole states in zinc-blende semiconductors in the spherical approximation. We have developed an efficient numerical method to solve the two coupled BL differential equations. The study of three different cases, namely the QD, the neutral acceptor and the free MP, shows that the present method always gives an increase of the MP energy with respect to the usual simplified model assuming a single parabolic band of mass m_h and a modified exchange parameter $\rho\beta$. In particular, there is no optimum (ρ, m_h) pair to fit the temperature dependence of the MP energy. It is also clear that a natural choice for m_h in a given material depends on the problem to be solved (see table 3); this is particularly difficult in the free MP case since there is no binding in the absence of exchange coupling. We conclude that the new method we propose is the most reliable one for zinc-blende materials.

We have already obtained an excellent *parameter free* fit of the A^0 MP energy versus T in diluted systems. The strongest discrepancy between the present model and the (usual) simplified one is expected in QDs. Experimental data in a zinc-blende QD are highly desirable.

Appendix A

The numerical calculations are performed as follows: the r space is divided into intervals of length δ. For a QD of radius R, δ is typically $R/100$. For a 3D problem, e.g. the neutral acceptor, δ is at least one-20th of the Bohr radius a_B and r goes to r_M, at least $5\ a_B$. Through this discretization, a second-order differential equation for a function f of a single variable r reduces to a linear relation between the values of f at three consecutive points: $r = (i-1)\delta$, $i\delta$ and $(i+1)\delta$. In the case of the system of two coupled differential equations $(12a, b)$, we get a system of two linear equations between the values of f and g at three consecutive points corresponding to indices $i-1, i, i+1$. A correct behaviour near the origin [22] imposes $f(0) = 1$ and $g(0) = 0$; the value of $f(\delta)$ can be obtained by a development (for the acceptor, we obtain $f(\delta) = 1 - \delta(1-\mu^2)$ and for the hole localization in a nanocrystal $f(\delta) = 1 - E\delta^2/6$) and we set $g(\delta) = \alpha$, α being a parameter we shall determine later. So, the next values of f and g are obtained step by step by solving a system of two linear equations. The goal is to choose the parameters E and α such that $f(r)$ and $g(r)$ have the correct behaviour at $r = R$ (or $r = r_M$), with the additional condition that they have no node in the range $0 < r < R$. One can define two quantities, F and G which measure the distance of f and g from the required behaviour at $r = R$ (in the case of a QD, one can take $F = f(R)$ and $G = g(R)$ since we aim at $f(R) = 0$ and $g(R) = 0$; for A^0, since for large r $f(r) \sim \exp(-r\sqrt{E})$ and $g(r) \sim r\exp(-r\sqrt{E})$, we take $F = f(r_M) - f(r_M - \delta)\exp(-\delta\sqrt{E})$ and $G = g(r_M) - g(r_M - \delta)(r_M - \delta)\exp(-\delta\sqrt{E})/r_M)$. F and G are functions of E and α. We start from approximate values E_0 and α_0, obtained

by trial, such that $|F|$ and $|G|$ are smaller than 0.1 ; then we perform the calculation for two other points not aligned with the previous one in the (E, α) parameter space, for example $(E_0 + \delta E, \alpha_0)$ and $(E_0, \alpha E_0 + \delta\alpha)$. Then, from these three values of F and G, one can determine by a linear extrapolation the two lines L_F and L_G in the parameter space where we have respectively $F(E, \alpha) = 0$ and $G(E, \alpha) = 0$ (see figure A1). The intersection between L_F and L_G gives the next values (E_1, α_1) to be used in the calculation. A few iterations using decreasing values of δE and $\delta\alpha$ are enough to push $|F|$ and $|G|$ below 10^{-6}. The pair (E_i, α_i) tends towards the exact value when $E_i - E_{i-1}$ and $\alpha_i - \alpha_{i-1}$ tend towards zero, since in this limit the linear extrapolation becomes exact.

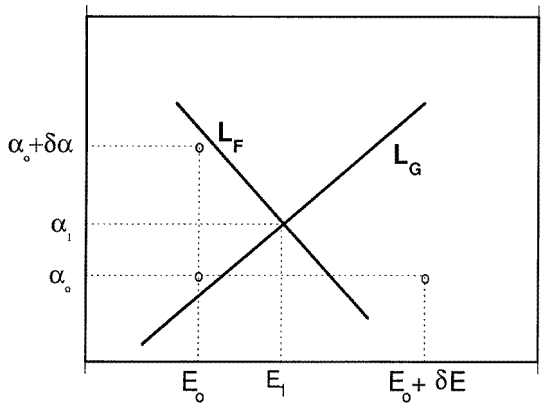

Figure A1. A sketch of the procedure described in appendix A to obtain the next (E_1, α_1) pair from the pair (E_0, α_0).

This procedure can be used if the potential is known from the beginning. For the MP case, we first solve (12*a*, *b*) with $V_{mag}(r) = 0$. Using the $f(r)$ and $g(r)$ thus obtained, we compute $B_{eff}(r)$ in (7) and then $V_{mag}(r)$ from (13) for the largest T value of interest. Then we solve again (12*a*, *b*) including $V_{mag}(r)$, thus obtaining a new pair of functions $f(r)$ and $g(r)$. Two or three iterations are sufficient to obtain good convergence. Computation is then carried out for decreasing values of T down to zero.

Appendix B

We examine now the behaviour of the system of equations (12*a*, *b*) for $V(r) = 0$ submitted to a perturbation $\varepsilon U(r)$, ε being the small parameter.

Assuming $f(r) = f_0(r) + \varepsilon f_1(r) + \cdots, g(r) = g_0(r) + \varepsilon g_1(r) + \cdots$ and $E = E_0 + \varepsilon E_1 + \cdots$ we obtain after substitution in (12*a*, *b*) from the ε terms (we take here $\hbar^2\gamma_1/2m_0 = 1$)

$$[\mathrm{d}^2/\mathrm{d}r^2 + (2/r)\,\mathrm{d}/\mathrm{d}r + E_0]f_1(r) - \mu[\mathrm{d}^2/\mathrm{d}r^2 + (5/r)\,\mathrm{d}/\mathrm{d}r + 3/r^2]g_1(r) = [U(r) - E_1]f_0(r) \tag{B1}$$

$$[\mathrm{d}^2/\mathrm{d}r^2 + (2/r)\,\mathrm{d}/\mathrm{d}r - 6/r^2 + E_0]g_1(r) - \mu[\mathrm{d}^2/\mathrm{d}r^2 - (1/r)\,\mathrm{d}/\mathrm{d}r]f_1(r) = [U(r) - E_1]g_0(r). \tag{B2}$$

Let us remark that we cannot have $f_1(r) = 0$ and $g_1(r) = 0$ since we would obtain two values for E_1, $\langle f_0|U|f_0\rangle/\langle f_0|f_0\rangle$ and $\langle g_0|U|g_0\rangle/\langle g_0|g_0\rangle$ which are obviously not equal, except for a uniform $U(r)$.

After multiplication on the left of (B1) by $f_0(r)$ and performing space integration, we obtain

$$\langle f_0|U(r) - E_1|f_0\rangle = \langle f_1|\mathrm{d}^2/\mathrm{d}r^2 + (2/r)\,\mathrm{d}/\mathrm{d}r + E_0|f_0\rangle \\ -\mu\langle g_1|\,\mathrm{d}^2/\mathrm{d}r^2 + (5/r)\,\mathrm{d}/\mathrm{d}r + (3/r^2)|f_0\rangle. \tag{B3}$$

(B3) can be transformed, using (12a):

$$\langle f_0|U(r) - E_1|f_0\rangle = \mu[\langle f_1|\mathrm{d}^2/\mathrm{d}r^2 + (5/r)\,\mathrm{d}/\mathrm{d}r + (3/r^2)|g_0\rangle \\ -\langle g_1|\mathrm{d}^2/\mathrm{d}r^2 + (5/r)\,\mathrm{d}/\mathrm{d}r + (3/r^2)|f_0\rangle]. \tag{B4}$$

In the same way, we obtain from (B2)

$$\langle g_0|U(r) - E_1|g_0\rangle = \mu[\langle g_1|\mathrm{d}^2/\mathrm{d}r^2 - (1/r)(\mathrm{d}/\mathrm{d}r)|f_0\rangle - \langle f_1|\,\mathrm{d}^2/\mathrm{d}r^2 - (1/r)(\mathrm{d}/\mathrm{d}r)|g_0\rangle]. \tag{B5}$$

Summing (B4) and (B5), with f_0 and g_0 obeying (4), we obtain

$$E_1 = \langle f_0|U(r)|f_0\rangle + \langle g_0|U(r)|g_0\rangle \\ -3\mu[\langle f_1|(2/r)\,\mathrm{d}/\mathrm{d}r + (1/r^2)|g_0\rangle - \langle g_1|(2/r)\,\mathrm{d}/\mathrm{d}r + (1/r^2)|f_0\rangle]. \tag{B6}$$

We assume that the second term in (B6) is small, some cancellation arising between the two cross terms, so we shall use

$$E_1 = \langle f_0|U(r)|f_0\rangle + \langle g_0|U(r)|g_0\rangle. \tag{B7}$$

The validity of (B7) was checked in the case of a square well potential of radius $R/5$. We have found that the numerical result exceeds the prediction of (B7) only for $\mu > 0.8$, the discrepancy being about 1.5% for $\mu = 0.95$.

In the case of a small magnetic potential in the linear regime, we can write $U(r) = |f_0(r)|^2 + \frac{1}{5}|g_0(r)|^2$ in (B1) and put $U(r)/5$ in (B2). Then, following the same derivation, we obtain (after dropping the index 0)

$$E_1 = \langle f|(|f|^2 + \tfrac{1}{5}|g|^2)|f\rangle + \tfrac{1}{5}\langle g|(|f|^2 + \tfrac{1}{5}|g|^2)|g\rangle. \tag{B8}$$

Since for $\mu = 0$ we obtain $E_0 = \langle f_0|f_0^2|f_0\rangle$ where the index refers now to $\mu = 0$, we obtain the expression of the enhancement factor $\eta = E_1/E_0$ in (18).

References

[1] Wolff P A 1988 *Diluted Magnetic Semiconductors (Semiconductors and Semimetals 25)* ed J K Furdyna and J Kossut (New York: Academic) ch 10

[2] Bhattacharjee A K and Benoit à la Guillaume C 1996 *Proc. 23rd Int. Conf. on the Physics of Semicond. (Berlin, 1996)* ed M Scheffler and R Zimmermann (Singapore: World Scientific) p 1469

[3] Mycielski J and Rigaux C 1983 *J. Physique* **44** 1041

[4] Bhattacharjee A K 1995 *Phys. Rev.* B **51** 9912

[5] Baldereschi A and Lipari N O 1973 *Phys. Rev.* B **8** 2697

[6] Efros A L 1992 *Phys. Rev.* B **46** 7448

[7] Richard T, Lefevbre P, Mathieu H and Allègre J 1996 *Phys. Rev.* B **53** 7287

[8] Ram-Mohan L R and Wolff P A 1988 *Phys. Rev.* B **38** 1330

[9] Heiman D, Isaacs E D, Becla P and Foner S 1987 *Phys. Rev.* B **35** 3307

[10] Lawaetz P 1971 *Phys. Rev.* B **4** 3460

[11] Le Si Dang 1997 *Phys. Rev.* B at press

[12] Bhattacharjee A K and Benoit à la Guillaume C, to be published

[13] Nhung T R, Planel R, Benoit à la Guillaume C and Bhattacharjee A K 1985 *Phys. Rev.* B **31** 2388

[14] Bugajski M, Becla P, Wolff P A, Heiman D and Ram-Mohan L R 1988 *Phys. Rev.* B **38** 10 512

[15] Janiszewski P 1990 *Proc. 20th Int. Conf. on the Physics of Semicond.* ed E M Anastassakis and J D Joannopoulos (Singapore: World Scientific) p 771

[16] Benoit à la Guillaume C, Semenov Yu G and Combescot M 1995 *Phys. Rev.* B **51** 14 124

[17] The use of a coupling constant λ is strictly valid only if the magnetization $M(H, T)$ is function of a single variable, i.e. $H/(T + T_0)$ when M is described by a modified Brillouin function. This is not the case if M is described by (14).
[18] The efficiency of the procedure described in appendix A is poor in the free MP case, especially for $\mu > 0.8$ and small values of the polaron energy.
[19] Berkovskaya Yu F, Gel'mont B L and Tsidil'kovskii E I 1998 *Fiz. Tekh. Poluprovodn.* **22** 855 (Engl. transl. *Sov. Phys.–Semicond.* **22** 539)
[20] Linnik T L, Rubo Yu G and Sheka V I 1996 *Pis. Zh. Eksp. Teor. Fiz.* **63** 209 (Engl. transl. *JETP Lett.* **63** 222)
[21] Scalbert D, Cernogora J, Benoit à la Guillaume C and Nawrocki M 1988 *Phys. Rev.* B **38** 13 246
Bhattacharjee A K 1997 *Phys. Rev.* B **35** 9108
[22] Mendelson K S and James H M 1964 *J. Phys. Chem. Solids* **25** 729